Human Molecular Genetics, 2008, Vol. 17, No. 24 ***3975–3986***
doi:10.1093/hmg/ddn301
Advance Access published on September 16, 2008

Molecular and cellular adaptations to chronic myotendinous strain injury in *mdx* mice expressing a truncated dystrophin

Glen B. Banks[1], Ariana C. Combs[1], Joel R. Chamberlain[2] and Jeffrey S. Chamberlain[1,2,3,*]

[1]Department of Neurology, Senator Paul D. Wellstone Muscular Dystrophy Cooperative Research Center, [2]Department of Medicine and [3]Department of Biochemistry, University of Washington, Seattle, WA 98195, USA

Received June 30, 2008; Revised August 21, 2008; Accepted September 15, 2008

Myotendinous strain injury is the most common injury of human skeletal muscles because the majority of muscle forces are transmitted through this region. Although the immediate response to strain injury is well characterized, the chronic response to myotendinous strain injury is less clear. Here we examined the molecular and cellular adaptations to chronic myotendinous strain injury in *mdx* mice expressing a micro-dystrophin transgene (microdystrophin$^{\Delta R4-R23}$). We found that muscles with myotendinous strain injury had an increased expression of utrophin and α7-integrin together with the dramatic restructuring of peripheral myofibrils into concentric rings. The sarcolemma of the microdystrophin$^{\Delta R4-R23}$/*mdx* gastrocnemius muscles was highly protected from experimental lengthening contractions, better than wild-type muscles. We also found a positive correlation between myotendinous strain injury and ringed fibers in the HSA^{LR} (human skeletal actin, long repeat) mouse model of myotonic dystrophy. We suggest that changes in protein expression and the formation of rings are adaptations to myotendinous strain injury that help to prevent muscle necrosis and retain the function of necessary muscles during injury, ageing and disease.

INTRODUCTION

Myotendinous junction (MTJ) is the major site of force transfer in skeletal muscle (1). This junction is a highly specialized interface where the tendon extends deep folds into the muscle to minimize membrane stress under shear (1). Many spectrin-based cytoskeletal proteins, intermediate filaments and integrins form the structural scaffold that connects the muscle to the tendon (2). Despite the molecular and cellular specializations of the MTJ, myotendinous strain injury is the most common form of muscle injury in humans (3–6). Myotendinous strain injury is caused by over-stretching of the muscle and is clinically categorized into stretch injury (first degree), partial tears (second degree) and complete rupture or avulsion (third degree) (7).

Acute stretch injury of skeletal muscles has been well characterized. Acute stretch of normal muscles leads to tears in the sarcolemma and within the contractile sarcomeres directly adjacent to the MTJ (8). Disuse atrophy of skeletal muscles leads to a reduction in the amount of junctional folding and is a common site of injury when the muscles are re-loaded (1). Acute stretch injury also leads to mechanotransduction where activation of α7-integrin expression reduces the phosphorylation of the mitogen-activated protein (MAP) kinase signaling pathway (9). The MAP kinase pathway is activated by mechanical stretch of the muscles and is implicated in promoting muscle damage responses (9–11). However, the molecular and cellular responses to chronic myotendinous strain injury are less clear. Tendon avulsion in several different animal models can lead to ringed fibers (12–14). Ringed fibers (also known as ringbinden, annular ring formation or spiral annulets) are where the peripheral myofibrils within a muscle fiber form concentric rings around the central myofibrils (15). Ringed fibers are found in most human muscles, especially in those muscles that do not attach from bone to bone (such as ocular, uvula, tongue and diaphragm muscles) (13). Ringed fibers become more prominent with age (13,16) and are a common (30–70%) histopathological feature of all types of muscular dystrophy and myopathy (15). However, the natural cause,

*To whom correspondence should be addressed at: Jeffrey S. Chamberlain, Rm K243b HSB, Box 357720, University of Washington School of Medicine, 1959 NE Pacific Street, Seattle, WA 98195-7720, USA. Tel: +1 2066166645; Fax: +1 2066168272; Email: jsc5@u.washington.edu

mechanical properties and function of ringed fibers are not known.

Duchenne muscular dystrophy (DMD) is a lethal X-linked recessive disease caused by mutations in the 2.2 Mb dystrophin gene (17–19). In skeletal muscle, dystrophin provides a flexible connection between the cytoskeleton and the dystrophin glycoprotein complex at the MTJ (20–22). Dystrophin-deficient muscles are highly susceptible to contraction-induced injury and they undergo repeated cycles of necrosis and regeneration (18). Most prospective gene therapies for DMD require the generation of highly functional truncated dystrophins that prevent muscle degeneration (23). In the present study we found that a truncated microdystrophin$^{\Delta R4-R23}$ led to myotendinous pathology consistent with chronic myotendinous strain injury in the *mdx* mouse model of DMD. We suggest that myotendinous strain injury leads to molecular and cellular adaptations throughout the gastrocnemius muscle to help to protect the sarcolemma.

RESULTS

Effects of microdystrophin$^{\Delta R4-R23}$ transgene at the MTJ of *mdx* mice

We compared *mdx* mice expressing either microdystrophin$^{\Delta R4-R23}$ or minidystrophin (minidysGFP) transgenes (Fig. 1A) (24,25). Dystrophin is normally concentrated at the MTJ in skeletal muscle (Fig. 1B). We found that microdystrophin$^{\Delta R4-R23}$ and minidysGFP were also concentrated at the Achilles MTJ (Fig. 1B). Many of the junctional folds are present in *mdx* mice, but do not extend as far into the muscle at 3 months of age (Fig. 1B and E; $P < 0.001$) (26). We examined whether microdystrophin$^{\Delta R4-R23}$ and minidysGFP transgenes could maintain the Achilles MTJ in *mdx* mice at 3 months of age using electron microscopy (EM) and resin sections stained with toluidine blue ($n = 4$). The length of the junctional folds was restored in both microdystrophin$^{\Delta R4-R23}$/*mdx* and minidysGFP/*mdx* mice, with no significant difference in wild-type muscles ($n = 4$; Fig. 1B and E; $P > 0.05$). However, the most striking features of this region in microdystrophin$^{\Delta R4-R23}$/*mdx* mice were tears in the MTJs and tendon (Fig. 1B and C). These tears were associated with pathological changes such as degeneration of myofibrils and infiltration of adipocytes into the muscle–tendon area (Fig. 1B and C). Serial sections through the MTJ and tendon showed that the tears were localized (data not shown). The physical disruption was associated with a rippled appearance of the MTJ in ~70% of muscle fibers ($n = 4$; Fig. 1D). Toward the ends of the muscle fibers the I-bands in the myofibrils were absent and the Z-lines were thickened (Fig. 1B and D). We examined an additional five mice between 7 weeks and 6 months of age and found injury throughout this time frame showing the physical disruption was chronic (data not shown). This phenotype depended on the muscle groups that were examined because we found no evidence of tearing at the lateral MTJ in diaphragm muscles of these same transgenic mice ($n = 4$). We also looked for tears in the Achilles MTJ from wild-type, *mdx*, or minidysGFP/*mdx* mice and found none ($n = 4$). Thus, expression of the microdystrophin$^{\Delta R4-R23}$ transgene in *mdx* mice was associated with chronic partial tears in the Achilles MTJ and tendon consistent with second-degree myotendinous strain injury (7).

Molecular changes in muscles with chronic myotendinous strain injury

Because the microdystrophin$^{\Delta R4-R23}$/*mdx* mice have few central nuclei (Supplementary Material, Fig. S1) and perform better than wild-type mice on forced exercise tests (24), we considered that there might exist molecular adaptations to the myotendinous strain injury. We examined the location and expression of α-dystrobrevin, α7-integrin and utrophin because these proteins each maintain MTJ fold structure and help to protect skeletal muscles from degeneration (27–29). We examined the location of these proteins in longitudinal sections of the Achilles MTJ and examined levels of expression in immunoblots from whole gastrocnemius muscle preparations. α-dystrobrevin was localized to the MTJ in *mdx* mice, but the expression of α-dystrobrevin was reduced compared with wild-type mice (Fig. 2; Table 1). α7-integrin was localized to the *mdx* Achilles MTJ in qualitatively higher concentrations, but expression in whole muscle preparations in immunoblots was unchanged at 3 months of age (Fig. 2; Table 1). Utrophin was located at the MTJ and its expression was elevated by ~30% in *mdx* muscles (Fig. 2; Table 1). We found α-dystrobrevin, α7-integrin and utrophin were concentrated at the Achilles MTJ in *mdx* mice expressing microdystrophin$^{\Delta R4-R23}$ and minidysGFP transgenes (Fig. 2A). The expression of α-dystrobrevin was increased in the microdystrophin$^{\Delta R4-R23}$/*mdx* gastrocnemius and diaphragm muscles (Fig. 2; Table 1). The expression of α7-integrin was increased by 30% and utrophin expression was increased by 14% in the microdystrophin$^{\Delta R4-R23}$/*mdx* gastrocnemius muscles with myotendinous strain injury. The expression of α7-integrin and utrophin was unchanged in the diaphragm of microdystrophin$^{\Delta R4-R23}$/*mdx* transgenic mice compared with wild-type mice (Fig. 2; Table 1). We found no change in expression in both the gastrocnemius and diaphragm muscles in the minidysGFP transgenic mice, which do not have torn MTJs (Fig. 2; Table 1). Total protein was equivalent for all samples as indicated by detection of α-actin as a Control for gel loading (Fig. 2B). Together, these results show that muscles with myotendinous strain injury have increased expression of α7-integrin and utrophin in microdystrophin$^{\Delta R4-R23}$/*mdx* mice.

Cellular changes in muscles with chronic myotendinous strain injury

The muscle morphology in *mdx* mice expressing truncated dystrophins has previously been shown in frozen sections stained with hematoxylin and eosin (24,30,31). Hematoxylin and eosin can detect overt signs of muscle pathology, but are limited in detailing more intricate structural alterations in the muscle. Here, we examined the muscles ultrastructure in transverse EM and resin sections stained with toluidine blue in microdystrophin$^{\Delta R4-R23}$/*mdx* mice ($n = 4$). We found ringed fibers in *mdx* muscles expressing the microdystrophin$^{\Delta R4-R23}$ transgene (Fig. 3A–C). The ringed fibers expressed desmin (Fig. 3C), similar to the ringed fibers experimentally induced

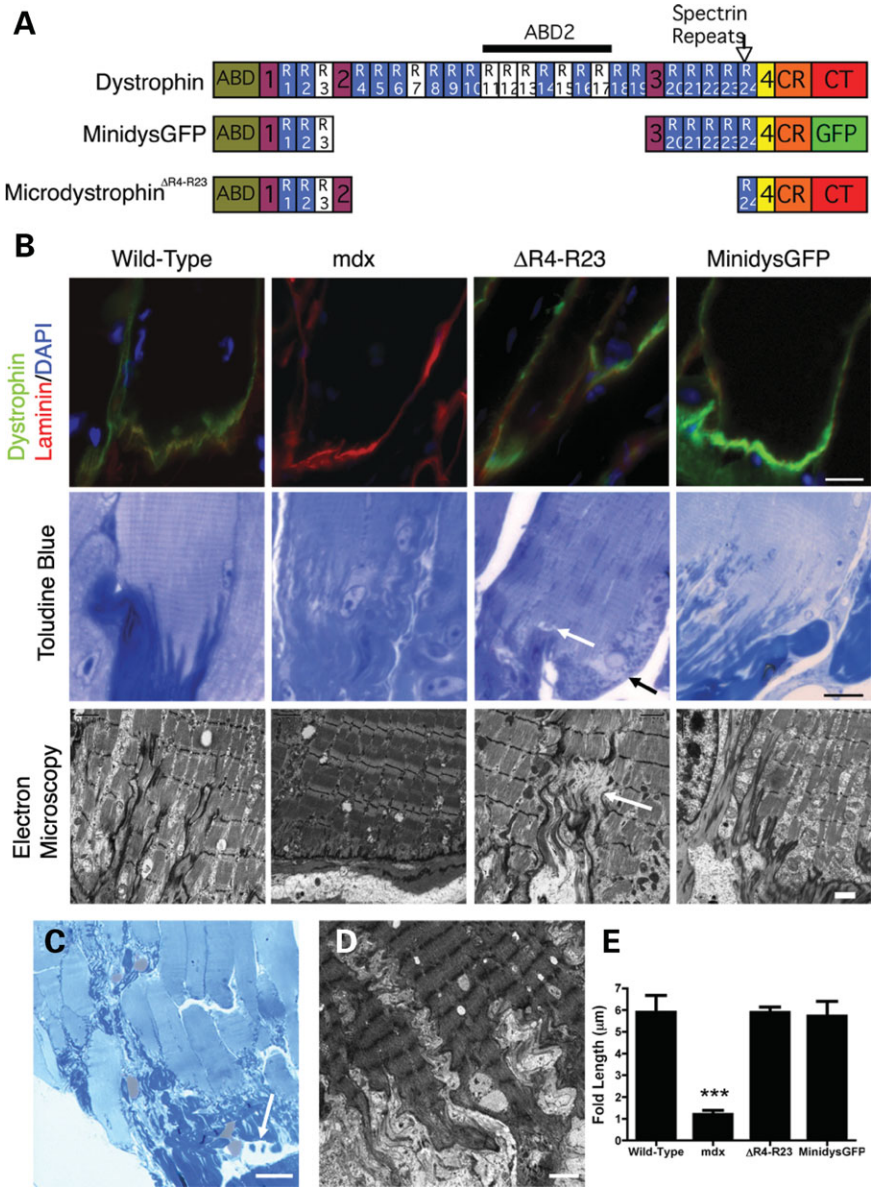

Figure 1. Chronic myotendinous strain injury at the Achilles myotendinous junction (MTJ) in *mdx* mice expressing the microdystrophin$^{\Delta R4-R23}$ transgene. (**A**) The molecular structure of truncated dystrophins. Dystrophin contains two actin-binding domains (ABD), a large central rod domain, a cysteine-rich region (CR) and a C-terminal (CT) domain. The central rod domain is composed of four hinge regions and 24 spectrin-like repeats. The transgenes used in this study are shown below the full-length dystrophin. *Mdx* mice expressing microdystrophin$^{\Delta R4-R23}$ and minidysGFP (ΔH2-R19/ΔCT, GFP) transgenes have been published previously (24,25). MinidysGFP has an enhanced green fluorescence protein (GFP) in place of the CT domain. (**B**) Dystrophin, microdystrophin$^{\Delta R4-R23}$ and minidysGFP (all shown in green) concentrate in the MTJ in the gastrocnemius muscle with laminin (shown in red). Nuclei are stained with 4′,6-diamidino-2-phenylindole in blue. Toluidine blue images show that tears in the MTJ can associate with sites of myofibril degeneration. White arrows show sites of failure within the MTJ (B) and tendon (**C**) in microdystrophin$^{\Delta R4-R23}$/*mdx* mice. Black arrows show the accompanying pathology. (**D**) Electron microscopy images show a rippled appearance of the MTJs, thickened Z-lines and absence of I-bands in microdystrophin$^{\Delta R4-R23}$/*mdx* transgenic mice. (**E**) The mean ± SE length of folds at the Achilles MTJ. Note that the length of folds are reduced in *mdx* mice and restored by the truncated dystrophin transgenes. $^{***}P < 0.001$ compared with wild-type. Scale bar = 2 μm for electron microscopy images and 10 μm for other images.

by tendon avulsion (14,32). The frequency of ringed fibers varied between muscle groups (Fig. 3D). The highest occurrence was in the gastrocnemius (64%) and quadriceps (60%; Fig. 3D). There were few ringed fibers in the tibialis anterior (19%) and none in the diaphragm (Fig. 3D). We could not find any ringed fibers with central nuclei showing that ringed fibers were not associated with muscle degeneration (Fig. 3B; Supplementary Material, Fig. S1A). The rings extended throughout the middle of the muscle and usually began near the site of injury at the MTJ (Supplementary Material, Fig. S2A), but sometimes extended into the MTJ and the myomuscular junction (Supplementary Material, Fig. S2B and C). Ringed fibers are proposed to form in denervated or split fibers but we found no evidence of this in microdystrophin$^{\Delta R4-R23}$/*mdx* mice (Supplementary Material, Fig. S3) (33). We found no ringed fibers in the gastrocnemius

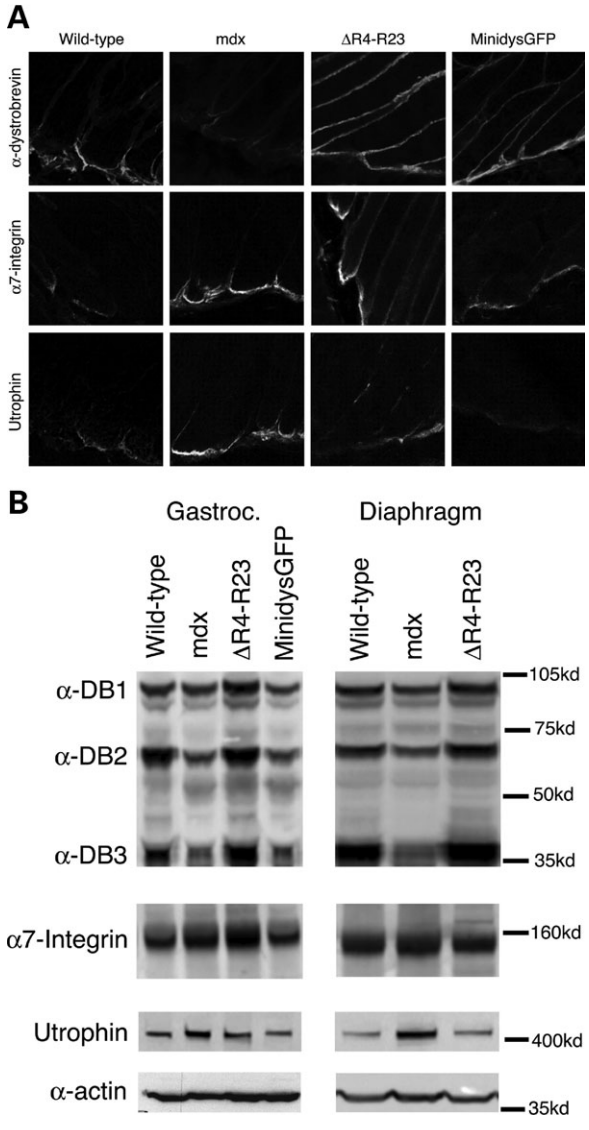

Figure 2. Expression and localization of α-dystrobrevin, α7-integrin and utrophin in wild-type, *mdx*, microdystrophin$^{\Delta R4-R23}$/*mdx* and minidysGFP/*mdx* mice. (**A**) Note that the truncated dystrophins restored α-dystrobrevin to the myotendinous junction (MTJ) in *mdx* mice. α7-integrin and utrophin were qualitatively increased in *mdx* and microdystrophin$^{\Delta R4-R23}$/*mdx* MTJs, but not in minidysGFP/*mdx* mice. (**B**) Expression of cytoskeletal proteins within the gastrocnemius and diaphragm muscles. All lanes were loaded equally as represented by α-actin. Note that α7-integrin and utrophin were increased in microdystrophin$^{\Delta R4-R23}$/*mdx* gastrocnemius muscles with myotendinous strain injury, but not in the diaphragm muscles that have no signs of myotendinous strain injury.

muscles from wild-type, *mdx* or minidysGFP/*mdx* mice (Fig. 3). Thus, ringed fibers were found in microdystrophin$^{\Delta R4-R23}$/*mdx* muscles with chronic myotendinous strain injury.

Mechanical properties of the gastrocnemius muscles

Muscle force production is generated in two directions (34–36). The first direction is longitudinally through the sarcomeres and the second is laterally from the peripheral sarcomeres to the basal lamina and along the tendon (34–36). The change in orientation of the peripheral myofibrils in

Table 1. Percent change in protein expression compared with wild-type muscles

	Gastrocnemius			Diaphragm	
	mdx	ΔR4–R23	MinidysGFP	*mdx*	ΔR4–R23
αDB1	−13	+45***	+1	−14*	+19**
αDB2	−40***	+10	−2	−27***	+15*
αDB3	−49***	+33*	−8	−43***	+18
α7-integrin	+3	+30***	−4	+5	−1
Utrophin	+30***	+16*	−2	+34*	−6

'+' is increased expression above wild-type; '−' is decreased expression below wild-type; significant difference compared with wild-type $^{*}P < 0.05$, $^{**}P < 0.01$, $^{***}P < 0.001$.

ringed fibers raises the possibility that the mechanical properties of the muscle could be altered in microdystrophin$^{\Delta R4-R23}$/*mdx* mice. To test this possibility we measured the force producing capacity of the gastrocnemius muscles ($n = 5–6$). We found that *mdx* gastrocnemius muscles were larger and developed reduced maximum and specific forces (force per cross-sectional area) compared with wild-type mice (Table 2), consistent with a previous report for the tibialis anterior muscles (24). The microdystrophin$^{\Delta R4-R23}$/*mdx* gastrocnemius muscles with many ringed fibers were smaller and had reduced maximum force compared with wild-type mice (Table 2), but exhibited significantly improved specific force compared with *mdx* muscle ($P < 0.001$ compared with *mdx* muscles; 91% of wild-type muscles; Table 2). We found no significant difference in muscle size, strength or specific force in minidysGFP mice compared with wild-type mice ($P > 0.05$; Table 2). Thus, the microdystrophin$^{\Delta R4-R23}$/*mdx* gastrocnemius muscles were smaller and weaker than wild-type muscles, but developed near normal levels of specific force despite having myotendinous strain injury and ringed fibers.

Susceptibility of gastrocnemius muscles to contraction-induced injury

Contraction-induced injury initiates muscle degeneration (reviewed in 37). The maximal force developed by skeletal muscles diminishes more rapidly in an eccentric stretch assay when the muscles are more susceptible to contraction-induced injury (31,38). We next examined whether the molecular and cellular adaptations to myotendinous strain injury had a protective effect on the gastrocnemius muscle in an eccentric stretch assay in microdystophin$^{\Delta R4-R23}$/*mdx* mice. The maximal force production depleted at a faster rate under strain in *mdx* gastrocnemius muscles compared with wild-type muscles ($n = 5–6$; Fig. 4A). Surprisingly, the muscles of microdystrophin$^{\Delta R4-R23}$/*mdx* gastrocnemius mice exhibited comparatively increased resistance to strain injury compared with wild-type muscles ($P < 0.001$; Fig. 4A). Maximal force production after strain was not different in minidysGFP muscles and wild-type muscles (Fig. 4A). These results show that microdystrophin$^{\Delta R4-R23}$/*mdx* gastrocnemius muscles were highly protected from contraction-induced injury in an eccentric stretch assay.

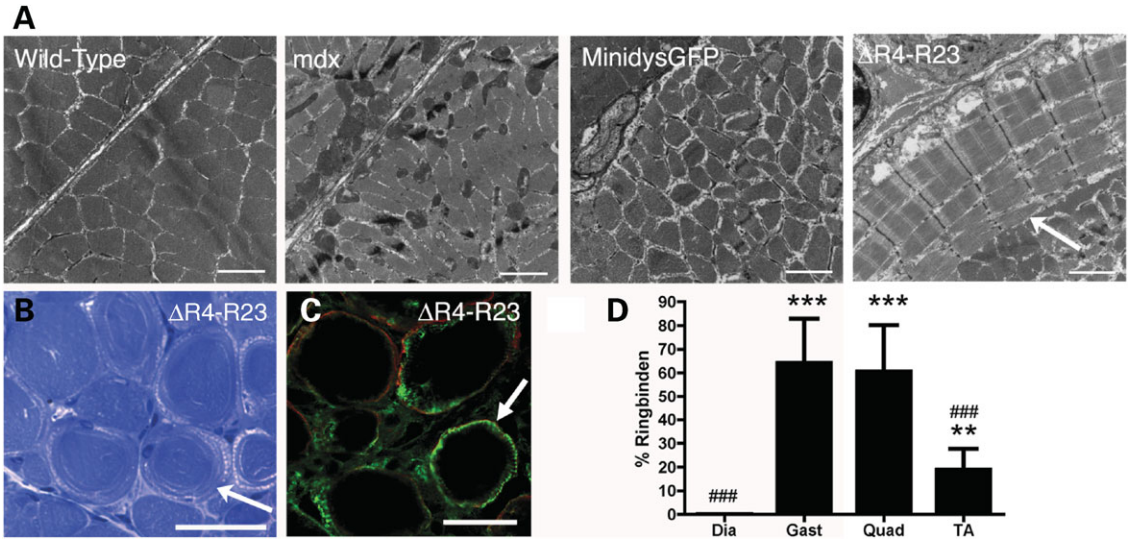

Figure 3. Ringed fibers in *mdx* mice expressing the microdystrophin$^{\Delta R4-R23}$ transgene. (**A**) Electron micrographs of two adjacent gastrocnemius muscle fibers from wild-type, *mdx*, microdystrophin$^{\Delta R4-R23}$/*mdx* and minidysGFP/*mdx* mice. Scale bars = 2 μm. (**B**) Ringed fibers in myofibers from microdystrophin$^{\Delta R4-R23}$/*mdx* gastrocnemius muscles stained with toluidine blue. Scale bar = 50 μm. (**C**) Transverse sections of muscle immunolabeled for desmin (green) and dystrophin (red). Scale bar = 50 μm. (**D**) Mean ± SD percentage of ringed fibers in various microdystrophin$^{\Delta R4-R23}$/*mdx* muscles. Scale bar = 50 μm. Arrows point to examples of rings. $^{***}P < 0.001$ and $^{**}P < 0.01$ compared with diaphragm; $^{\#\#\#}P < 0.001$ compared with gastrocnemius and quadriceps.

Table 2. Mechanical properties of the gastrocnemius muscles

	Muscle weight (mg)	Muscle length (mm)	Maximal force (kN)	Specific force (kN/m^2)
Wild-type	131 ± 6	14.4 ± 0.2	4451 ± 434	213 ± 21
mdx	177 ± 15***	14.7 ± 0.5	3285 ± 339**	124 ± 13***
ΔR4–R23	95 ± 10***	13.9 ± 0.5	3020 ± 266***	195 ± 15
MinidysGFP	132 ± 4	14.7 ± 0.6	4377 ± 383	213 ± 16

Values represent mean ± SD; significant difference compared with wild-type $^{**}P < 0.01$, $^{***}P < 0.001$.

We next examined whether the molecular and cellular changes in muscles with myotendinous strain injury could help to protect the sarcolemma from contraction-induced injury in microdystrophin$^{\Delta R4-R23}$/*mdx* gastrocnemius muscles. Evans blue dye (EBD) enters skeletal muscle when the sarcolemma is not intact (39). We delivered EBD intravenously to both wild-type and microdystrophin$^{\Delta R4-R23}$/*mdx* mice and examined the muscles after 33% strain ($n = 3$). We found no EBD in wild-type mice that were not stretched (Fig. 4B and C). However, eccentric stretch of wild-type muscles produced an acute strain injury that led to the influx of EBD into many fibers near the ends of the muscle (Fig. 4B and D). We found EBD at the MTJs and throughout a single fiber in microdystrophin$^{\Delta R4-R23}$/*mdx* muscles that had not been stretched (Fig. 4B and E), which is consistent with chronic injury in the MTJ (Fig. 1B). The number of muscle fibers with EBD after strain was unchanged in microdystrophin R4–R23/mdx gastrocnemius muscles (Fig. 4B and F and Supplementary Material, Table S1). EBD entered *mdx* muscle fibers before and after strain (Supplementary Material, Fig. S4 and Supplementary Material, Table S1). EBD was excluded from unstrained minidysGFP gastrocnemius muscle fibers as previously described (25), but entered the muscle fibers after 33% strain similar to wild-type mice (Supplementary Material, Fig. S4 and Table S1). Together, these results show that the microdystrophin$^{\Delta R4-R23}$/*mdx* gastrocnemius sarcolemma was highly protected from acute eccentric strain injury despite having chronic myotendinous strain injury.

Myotendinous strain injury correlates with ringed fibers in myotonic dystrophy

To further demonstrate the clinical significance of the correlation between myotendinous strain injury and ringed fibers in muscle disease we examined a mouse model of myotonic dystrophy (DM) (40). DM muscle tissue examined by light microscopy is characterized by the presence of ringed fibers in 70% of patients, muscles of variable size and some central nuclei in the absence of necrosis (15,40). Clinical features of DM include myotonia (muscle hyperexcitability), muscle wasting, and other seemingly unrelated phenotypes such as insulin resistance and cognitive defects (41). DM is caused by DNA repeat expansions that are expressed as part of an mRNA transcript that is not translated into protein. Instead, the repeat-containing mRNA accumulates in the nucleus as foci associated with proteins that are normally involved in the regulation of splicing of a variety of genes in the cell. The defects in splicing account for chloride channel depletion that cause myotonia (42) and may also explain the varied phenotypes associated with DM. Our interest in DM involved the disease aspects that contribute to ringed fibers, which are poorly understood. We chose the HSA^{LR} (human skeletal actin, long repeat) mouse model of DM that contains a long CTG repeat (~250) in the 3′-UTR of the human skeletal actin gene and recapitulates many phenotypic features of the human disease including myotonia and histological features such as ringed fibers (40). Examination of Achilles MTJs revealed regions of tearing associated with localized regions of pathology and infiltration of adipocytes

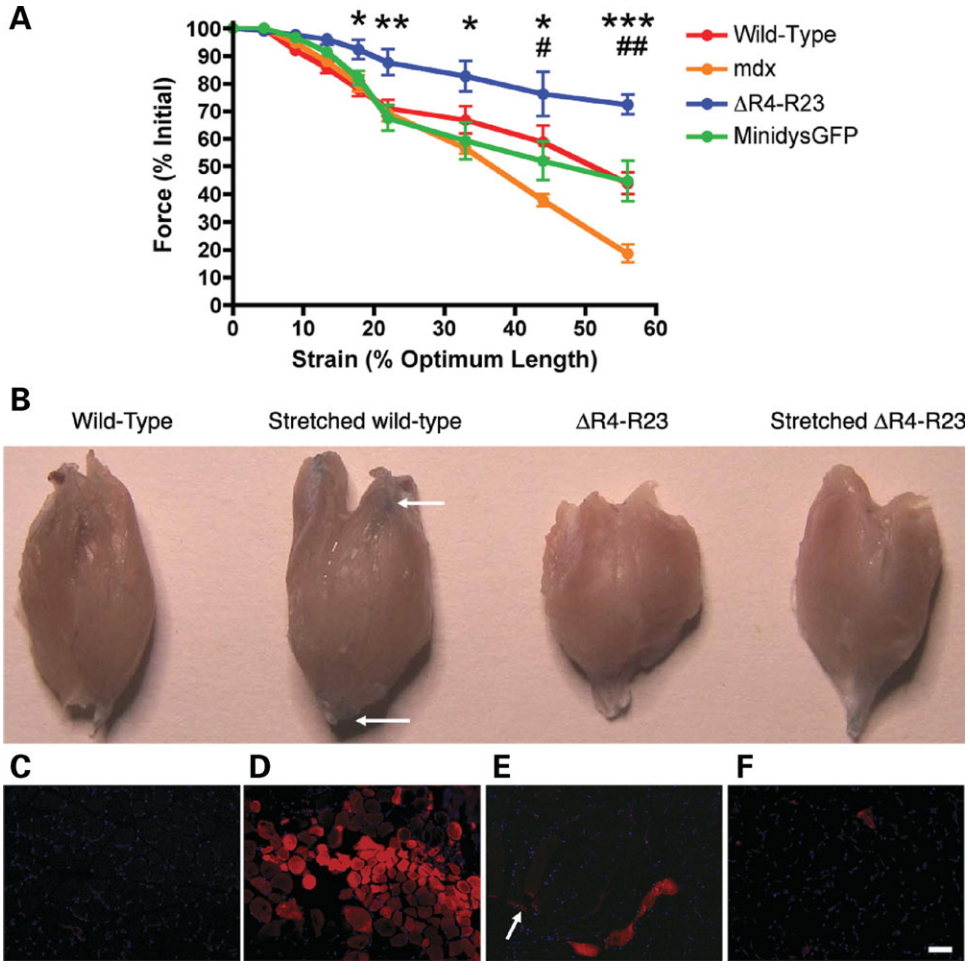

Figure 4. Gastrocnemius muscles expressing the microdystrophin$^{\Delta R4-R23}$ transgene were significantly protected from contraction-induced injury. (**A**) The contractile performance of gastrocnemius muscles immediately prior to increasing length changes during maximal force production for wild-type, *mdx*, microdystrophin$^{\Delta R4-R23}$/*mdx* transgenic and minidysGFP/*mdx* transgenic mice. Points represent the mean ± SD percentage of the initial optimal muscle contraction. Microdystrophin$^{\Delta R4-R23}$/*mdx* was significantly increased compared with wild-type ($^{*}P < 0.05$; $^{**}P < 0.01$; $^{***}P < 0.001$). *mdx* was significantly reduced compared with wild-type ($^{\#}P < 0.05$; $^{\#\#}P < 0.01$). (**B**) Gastrocnemius muscles after intravenous administration of Evans blue dye (EBD), before and after 33% stretch. EBD enters muscle fibers that have holes in the sarcolemma. Arrows point to EBD in fibers near the ends of the wild-type muscles after 33% stretch. (**C**) Cross-section of wild-type muscle showing no EBD without stretch-induced injury. Nuclei are shown in blue. (**D**) Cross-section of wild-type muscle stretched 33% beyond its optimal length. Note that many wild-type muscle fibers have EBD (in red) showing that contraction-induced injury tears the sarcolemma. (**E**) Representative longitudinal section of microdystrophin$^{\Delta R4-R23}$/*mdx* muscle that has not been stretched. Arrow points to EBD at the MTJs (myotendinous junctions). EBD is also present in a single muscle fiber. (**F**) Cross-section of microdystrophin$^{\Delta R4-R23}$/*mdx* muscle stretched 33% beyond its optimal length. Note the lack of EBD showing the sarcolemma was significantly protected from contraction-induced injury in the eccentric stretch assay. Scale Bar = 50 μm.

in ∼2% of the muscle fibers ($n = 3$; Fig. 5A). From these mice ∼3% of the gastrocnemius muscles had ringed fibers ($n = 3$; Fig. 5B and C). Thus, the relative number of regions with tears in the MTJ correlated positively with the ringed fibers in the HSA^{LR} mouse model of DM.

DISCUSSION

Microdystrophin$^{\Delta R4-R23}$ is a highly functional truncated dystrophin that is being developed in pre-clinical studies for gene therapy of DMD using rAAV. We found here that *mdx* mice expressing microdystrophin$^{\Delta R4-R23}$ were prone to disruption of the MTJ consistent with chronic myotendinous strain injury. Because the microdystrophin$^{\Delta R4-R23}$/*mdx* mice have few central nuclei and perform better than wild-type mice on forced exercise tests (24), we considered that there might exist molecular and cellular adaptations to the myotendinous strain injury. We found that myotendinous disruption correlated with an increase in α7-integrin and utrophin expression compared with wild-type muscles. In addition we found that myotendinous strain injury correlated with ringed fibers. These muscles were highly protected from contraction-induced injury in an acute eccentric stretch assay, which could explain the lack of muscle degeneration in microdystrophin$^{\Delta R4-R23}$/*mdx* mice (24). This observation prompted us to propose a model whereby chronic myotendinous strain injury leads to both molecular and cellular adaptations that help to protect the sarcolemma from further contraction-induced injury (Fig. 6).

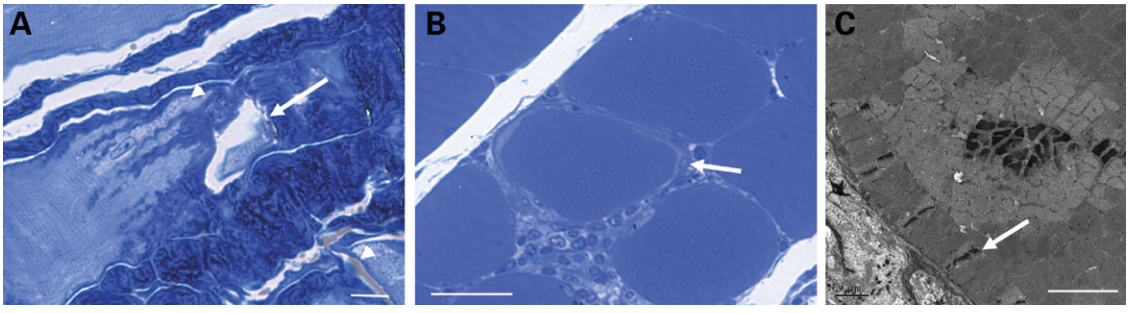

Figure 5. Correlation between myotendinous strain injury and ringed fibers in the HSA^{LR} (human skeletal actin, long repeat) mouse model of DM (myotonic dystrophy). (**A**) Longitudinal resin section of the Achilles MTJ (myotendinous junction) stained with toluidine blue. Arrow points to a partial tear. Arrowheads point to accompanying pathology and infiltration of adipocytes. Scale bar = 5 μm. (**B**) Transverse section of the gastrocnemius stained with toluidine blue. Scale bar = 20 μm. (**C**) Electron microscopy image of a ringed fiber. Scale bar = 2 μm. Arrows in (B) and (C) point to the rings.

Myotendinous strain injury

Myotendinous strain injury is the most common form of muscle injury in humans (3–6). Acute strain of skeletal muscle can lead to regional tears in the sarcolemma (Figs 4 and 6), tensile failure adjacent to the MTJs (8) and avulsion of the tendon (Fig. 6). We found partial tears in the Achilles MTJ and tendon of microdystrophin$^{\Delta R4-R23}$/*mdx* mice consistent with chronic second-degree myotendinous strain injury (Fig. 1). It is difficult to know whether the myotendinous disruption in microdystrophin$^{\Delta R4-R23}$/*mdx* mice resulted from an actual over-extension of the muscle. However, we do know that expression of the transgene alone is not sufficient to cause myotendinous disruptions because we found no disruption of the MTJs in the diaphragm muscles. Furthermore, the length of the junctional folds was normal in microdystrophin$^{\Delta R4-R23}$/*mdx* mice. Thus, the myotendinous pathology in microdystrophin$^{\Delta R4-R23}$/*mdx* mice was unlikely to result from defects in development or maturation. Furthermore, the tears in the MTJ and tendon together with degeneration of some myofibrils and infiltration of dark adipose cells into the muscle–tendon region are all consistent with chronic myotendinous strain injury. Based on these data we suggest that the Achilles heals of microdystrophin$^{\Delta R4-R23}$/*mdx* mice are more susceptible to myotendinous strain injury. To our knowledge, myotendinous strain injury described here in microdystrophin$^{\Delta R4-R23}$/*mdx* mice and the HSA^{LR} mouse model of DM have not been described previously in mice. The MTJs from *mdx* mice only have minor reductions in folding (1), which is similar to α-dystrobrevin (29) and α7-integrin (27) knockout mice. In addition, mice lacking both dystrophin and utrophin have a severe lack of junctional architecture where few sarcomeres make contact with the tendon (28). The reduction in folding within these genetically targeted mice most likely result from developmental and maintenance defects rather than strain injury (26). The lack of dystrophin, utrophin, α-dystrobrevin and α7-integrin does not appear to render MTJs more susceptible to strain injury in sedentary quadruped mice (1,27–29), but this could be different in bipedal humans. For instance, injury has been shown to begin at the MTJ in DMD patients (43,44). The myotendinous strain injury in microdystrophin$^{\Delta R4-R23}$/*mdx* mice suggests this truncated dystrophin is unable to maintain the Achilles MTJ during muscle force transfer. This suggests full-length dystrophin actively participates in force transfer at the MTJ. Forces transferred laterally through the dystrophin–glycoprotein complex to the interstitial matrix and ultimately to the tendon could also be abnormal in microdystrophin$^{\Delta R4-R23}$/*mdx* mice and this could contribute to myotendinous strain injury (45,46). Although less likely, an alternative hypothesis is that the ringed fibers prevent lateral force transmission between muscle fibers, which results in most of the forces extending to the MTJ within each muscle fiber rendering this region more susceptible to injury.

Molecular adaptations to chronic myotendinous strain injury

In the present study we found a clear association between increased α7-integrin and utrophin expression in the gastrocnemius muscles with myotendinous strain injury. Both α7-integrin and utrophin expression were unchanged in the diaphragm muscles of microdystrophin$^{\Delta R4-R23}$/*mdx* mice that did not have myotendinous strain injury. These results suggest that the increases in protein expression are molecular adaptations to myotendinous strain injury. However, it is also possible that microdystrophin could be exerting its effects at the sarcolemma to increase the expression of these proteins throughout the gastrocnemius muscle.

The increased expression of α7-integrin in muscles with myotendinous strain injury in microdystrophin$^{\Delta R4-R23}$/*mdx* mice is consistent with that found in muscles after stretch injury, exercise-induced injury and transection injury (9,47,48). α7-integrin links extracellular laminin to intracellular filamentous actin to help to prevent muscle degeneration (49) and maintains the folds at the MTJ (27). α7-integrin is a mechanical transducer that provides resistance to injury, possibly by reducing phosphorylation of the MAP kinase signaling pathway (9). The MAP kinase pathway is activated by mechanical stretch of the muscles and is implicated in promoting muscle damage responses (9–11). Thus, an increase in α7-integrin expression in microdystrophin$^{\Delta R4-R23}$/*mdx* gastrocnemius muscles could maintain the MTJ folds and help to protect the sarcolemma from contraction-induced injury.

The utrophin A isoform was also selectively increased in the gastrocnemius muscles of microdystrophin$^{\Delta R4-R23}$/*mdx* mice with myotendinous strain. Utrophin is a homolog of

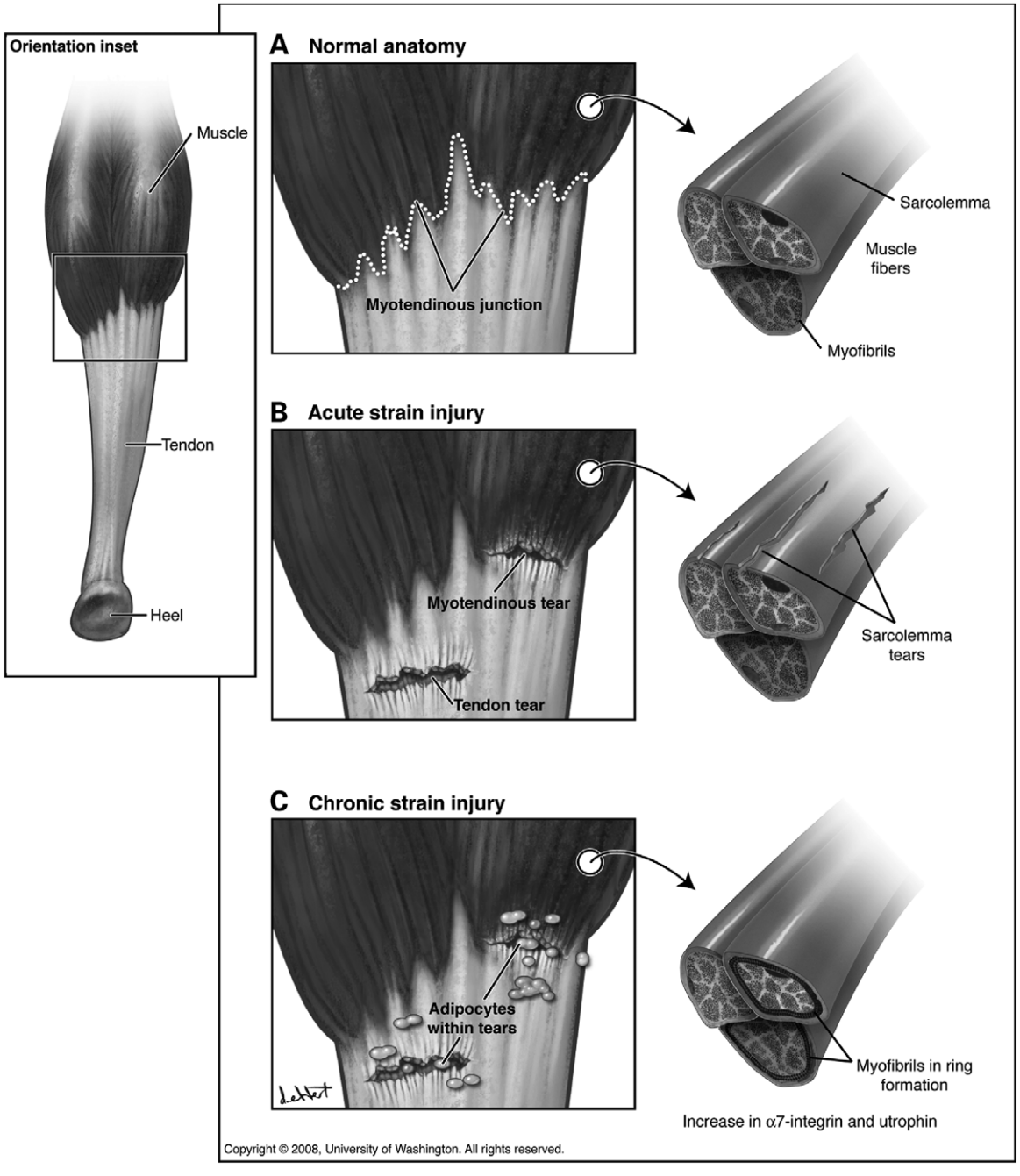

Figure 6. Model of acute and chronic myotendinous strain injury. Details are described in Discussion.

dystrophin that is up-regulated in *mdx* mice (50,51). The utrophin A isoform is normally found at the neuromuscular synapse and MTJs of wild-type mice (28,52–54). Utrophin partially restores the dystrophin–glycoprotein complex to the sarcolemma and partially protects muscles from contraction-induced injury in *mdx* mice (28,53,54). Genetic knockout of both dystrophin and utrophin leads to increased muscle necrosis, fewer folds at the MTJs and premature death (28,54). Therefore, the up-regulation of utrophin throughout the gastrocnemius muscles could compensate for the impaired functional capacity of microdystrophin$^{\Delta R4-R23}$ to help to prevent contraction-induced injury and restore MTJ folds.

α-Dystrobrevin expression is associated with reduced muscle necrosis and promotes the maturation of folds at the MTJ (29). α-dystrobrevin was increased in microdystrophin$^{\Delta R4-R23}$/*mdx* muscles whether there was myotendinous strain injury or not (Fig. 2; Table 1). Thus, we cannot conclude whether myotendinous strain leads to an increase in α-dystrobrevin expression. Interestingly, α-dystrobrevin expression was not increased in minidysGFP/*mdx* muscles. α-dystrobrevin binds directly to the C-terminal domain of

dystrophin (55), but remains on the sarcolemma in *mdx* mice expressing the ΔCT-dystrophin transgene (56). The increased expression of α-dystrobrevin in microdystrophin$^{\Delta R4-R23}$/*mdx* mice may reflect the increased expression of microdystrophin$^{\Delta R4-R23}$ (24), which allows more direct binding sites for α-dystrobrevin at the sarcolemma. The C-terminal domain of dystrophin is replaced by GFP (green fluorescence protein) in minidysGFP and consequently may not have an increased number of direct binding sites for α-dystrobrevin to stay at the sarcolemma, and the GFP moiety might also sterically hinder the association of α-dystrobrevin with the DGC (Fig. 1A) (25). The increased expression of α-dystrobrevin in the gastrocnemius muscles could help to protect the sarcolemma from contraction-induced injury and maintain the MTJ in microdystrophin$^{\Delta R4-R23}$/*mdx* mice.

Cellular adaptations to chronic myotendinous strain injury

We suggest that chronic myotendinous strain injury leads to ringed fibers in microdystrophin$^{\Delta R4-R23}$/*mdx* mice and the HSA^{LR} mice. We found a correlation between myotendinous strain injury and ringed fibers in the gastrocnemius muscles (Figs 1, 2 and 5). This is further supported by the lack of strain injury and ringed fibers in the diaphragm of microdystrophin$^{\Delta R4-R23}$/*mdx* mice. Our results are consistent with previous studies that show experimental tendon avulsion and muscle transection leading to the formation of ringed fibers (12–14). However, it is also possible that a local effect of microdystrophin$^{\Delta R4-R23}$ at the sarcolemma could lead to ringed fibers.

Skeletal muscles with many ringed fibers were highly protected from contraction-induced injury (Fig. 4). Normally, the peripheral sarcomeres align between muscle fibers to coordinate muscle contraction between motor units (35,45,46). This coordinate contraction allows the generation of lateral forces to the sarcolemma and extracellular matrix (35,45,46). Most of these forces are ultimately transferred to the tendon (35). Our results are consistent with this model in that the formation of rings isolates the fibers. This has the likely effect of reducing the transmission of lateral forces between fibers to minimize transmission of forces to the tendon (Table 1), and protect the sarcolemma from contraction-induced injury (Fig. 4). This model could explain why ringed fibers in humans become more prominent during injury, ageing and disease (13,15,16,57,58). It will be interesting to examine whether changes in compliance of the MTJ in microdystrophin$^{\Delta R4-R23}$/*mdx* mice could help to protect the muscles from further contraction-induced injury.

MATERIALS AND METHODS

Mice

We utilized C57Bl/10 wild-type mice, *mdx*^{4Cv} mice and *mdx* mice expressing microdystrophin$^{\Delta R4-R23}$ and minidysGFP transgenes (24,25). The transgenes utilized a human skeletal α-actin promoter for expression. We also utilized the HSA^{LR} mouse model of DM that was on an Friend leukemia Virus B background (40). Mice were genotyped as previously described (24,25,40). All experiments are in accordance with the Institution of Animal Care and Use Committee of the University of Washington.

Gross muscle morphology

Gross muscle morphology was analyzed as previously described (24,31). Primary antibodies included α2-chain of laminin (1:800; Sigma), N-terminus of dystrophin (1:800; 59), and the rod domain of dystrophin (Dys1; 1:20; Novocastra), α-dystrobrevin (1:200; Signal transduction), α7-integrin (1:2000; gift from Dean Burkin, University of Nevada), utrophin A (1:300; gift from Stanley Froehner, University of Washington), and desmin (1:100; Sigma). Secondary antibodies included Alexa 488, Alexa 594 rabbit polyclonal or Alexa 488 mouse monoclonal secondary antibodies (Molecular Probes; 1:800). Fluorescent sections were imaged using a Nikon eclipse E1000 fluorescent microscope (Nikon; NY, USA). The images of Figure 3C were viewed with a Leica SL confocal microscope (Leica SL, Exton PA) and captured using QIcam digital camera and processed using Qcapture Pro (Media Cybernetics Inc.).

Electron microscopy

Small (~2 mm^3) regions of diaphragm, tibialis anterior and quadriceps muscles were dissected and fixed in half-strength Karnovskys fixative for at least 24 h at 4°C. The entire gastrocnemius muscle was fixed in half-strength Karnovskys fixative in its optimal position while attached to the bone for at least 12 h at 4°C prior to dissection. The muscles were fixed on the bone so that none of the pathological features resulted from injury during surgery or processing. In each sample that we found a space between muscles, which can be caused by expanding and contracting tissues during embedding, we only considered tears in the tissues an injury in light of other pathological features such as myofibril degeneration and infiltration of dark fat cells that cannot occur after fixation (Figs 1 and 5). After fixation, muscles were washed in 0.1 M cacodylate buffer, post-fixed in 1% osmium tetroxide/cacodylate buffer for 2–3 h, washed in 0.1 M cacodylate buffer, dehydrated through ethanol into Epon, embedded, and polymerized at 60°C overnight. Thick 1 μm sections were cut and stained with toluidine blue. Ultra thin sections were cut between 70 and 100 nm and stained with saturated aqueous uranyl acetate and Reynolds lead citrate and viewed with a JEOL 1010 Transmission Electron Microscope (JEOL USA, Inc., MA, USA). Images were photographed with a wide-angle 1024 × 1024 Gatan 792 Multiscan 600W CCD camera (Gatan, Inc., CA, USA). The junctional folds were measured from $n = 4$ mice at 3 months of age using Image J (NIH) and compared using Students *t*-test (Prism).

Immunoblotting

For immunoblots, gastrocnemius and diaphragm muscles from 5-month-old mice were ground in liquid nitrogen and homogenized in extract buffer (50 mM Tris–HCl, 150 mM NaCl, 0.2% SDS (sodium dodecyl sulfate), 24 mM Na Deoxycholate, 1% NP40, 47.6 mM Na Fluoride, 200 mM Na Orthovanadate, Roche). Protein concentration of whole muscle was

determined by Coomassie Plus Bradford Assay (Pierce). Equal amounts of protein (20 μg) were resolved on a 4–12% SDS-polyacrylamide gel. The blots were incubated in rabbit polyclonal antibodies to α7-integrin (1:2000; gift from Dean Burkin, University of Nevada) and utrophin (1:1000; gift from Stanley Froehner, University of Washington), and mouse monoclonal antibodies to α-actin (1:500; Sigma Aldrich, St Louis, MO, USA) and α-dystrobrevin (1:1000; BD Transduction Labs). These antibodies were detected with donkey anti-rabbit immunoglobulin horse radish peroxidase (IgG HRP) or donkey anti-mouse IgG HRP (1:50 000; Jackson ImmunoResearch Labs). The blots were developed with ECL Plus and scanned with the Storm 860 imaging system (Amersham Biosciences). The band intensity was compared between $n = 8$ wild-type, *mdx*, microdystrophin$^{\Delta R4-R23}$/*mdx*, and $n = 7$ minidysGFP/*mdx* gastrocnemius muscles. The band intensity was also compared between $n = 7$ wild-type, *mdx*, microdystrophin$^{\Delta R4-R23}$/*mdx* diaphragm muscles (ImageQuant 5.1; Amersham Biosciences). Statistical differences were measured using non-parametric Students *t*-tests (Prism).

Quantitation of ringed fibers

We quantitated the number of ringed myofibers in EM images and thick (1 μm) toluidine blue sections from at least four animals per group. At least 300 muscle fibers from four diaphragm, gastrocnemius, quadriceps and tibialis anterior muscles were examined from microdystrophin$^{\Delta R4-R23}$/*mdx* transgenic mice. Approximately 560 muscle fibers from four gastrocnemius muscles were examined from HSA^{LR} mice.

Muscle physiology

Muscle physiology was performed as previously described (38), with minor modifications. Briefly, $n = 5$ 5-month-old wild-type, *mdx*, microdystrophin$^{\Delta R4-R23}$/*mdx*, minidysGFP/*mdx* mice were anesthetized with 2,2,2-tribromoethanol (Sigma) such that they were insensitive to tactile stimuli. Peak eccentric force of the gastrocnemius muscle was analyzed *in situ* via nerve stimulation. First we found the maximum force producing capacity of each gastrocnemius muscle at its optimum length according to maximal stimulation over 300 ms to elicit tetanic contraction. We then divided the peak force by the unit area of muscle to obtain specific force (kN/m^2). The equation is: Specific force = peak force × muscle length × 0.45 pennation × 1.04 density/muscle weight (60). Next, we measured the protection from contraction-induced injury. The force producing capacity of the muscle was measured immediately prior to increased length changes during maximal stimulation at 30 s intervals. The rate of length change was 2 lengths/s. To examine whether the sarcolemma was protected from contraction-induced injury we intravenously administered 0.5 mg of EBD per 10 g mouse body weight ∼20 min prior to the stretch protocol as previously described (61). The mice were stretched to 33% above their optimal length. EBD did not significantly alter the force producing capacity of the muscle. The stretched and non-stretched gastrocnemius muscles were frozen in 2-methylbutane cooled in liquid nitrogen ∼20 min after the stretch protocol (1 h total).

SUPPLEMENTARY MATERIAL

Supplementary Material is available at *HMG* Online.

FUNDING

This work was supported by grants from the National Institutes of Health NIH number AR044533. J.R.C. was funded by a fellowship from the Paul D. Wellstone Muscular Dystrophy Cooperative Research Center (MDCRC). G.B.B. was supported by a CJ Martin post-doctoral fellowship from the National Health and Medical Research Council of Australia (372212).

ACKNOWLEDGEMENTS

We are grateful to Leonard Meuse for animal husbandry, and Chamberlain lab members for critically reviewing the manuscript. We would also like to thank Franque Remington, Judith Bousman and Bobbie Schneider for electron microscopy, at the Fred Hutchinson Cancer Research Institute. In addition, we would like to thank Greg Martin at the Keck Imaging Center University of Washington for help with confocal microscopy. The HSA^{LR} mice were generously provided in collaboration with Charles Thornton, University of Rochester Paul D. Wellstone Muscular Dystrophy Cooperative Research Center (MDCRC).

Conflict of Interest statement. The authors have no conflicts of interest.

REFERENCES

1. Tidball, J.G. (1991) Force transmission across muscle cell membranes. *J. Biomech.*, **24** (Suppl. 1), 43–52.
2. Sheard, P., Paul, A. and Duxson, M. (2002) Intramuscular force transmission. *Adv. Exp. Med. Biol.*, **508**, 495–499.
3. Garrett, W.E. Jr (1988) Injuries to the muscle-tendon unit. *Instr. Course. Lect.*, **37**, 275–282.
4. Garrett, W.E. Jr, Nikolaou, P.K., Ribbeck, B.M., Glisson, R.R. and Seaber, A.V. (1988) The effect of muscle architecture on the biomechanical failure properties of skeletal muscle under passive extension. *Am. J. Sports. Med.*, **16**, 7–12.
5. Taylor, D.C., Dalton, J.D. Jr, Seaber, A.V. and Garrett, W.E. Jr (1993) Experimental muscle strain injury. Early functional and structural deficits and the increased risk for reinjury. *Am. J. Sports. Med.*, **21**, 190–194.
6. Weishaupt, D., Schweitzer, M.E. and Morrison, W.B. (2001) Injuries to the distal gastrocnemius muscle: MR findings. *J. Comput. Assist. Tomogr.*, **25**, 677–682.
7. Bencardino, J.T., Rosenberg, Z.S., Brown, R.R., Hassankhani, A., Lustrin, E.S. and Beltran, J. (2000) Traumatic musculotendinous injuries of the knee: diagnosis with MR imaging. *Radiographics*, **20** (Spec no.), S103–S120.
8. Law, D.J., Caputo, A. and Tidball, J.G. (1995) Site and mechanics of failure in normal and dystrophin-deficient skeletal muscle. *Muscle Nerve*, **18**, 216–223.
9. Boppart, M.D., Burkin, D.J. and Kaufman, S.J. (2006) Alpha7beta1-integrin regulates mechanotransduction and prevents skeletal muscle injury. *Am. J. Physiol. Cell. Physiol.*, **290**, C1660–C1665.
10. McCully, K.K. and Faulkner, J.A. (1985) Injury to skeletal muscle fibers of mice following lengthening contractions. *J. Appl. Physiol.*, **59**, 119–126.
11. Morgan, D.L. and Allen, D.G. (1999) Early events in stretch-induced muscle damage. *J. Appl. Physiol.*, **87**, 2007–2015.

12. Morris, W.R. (1959) Striated annulets (Ringbinden), their experimental production in mammalian muscle. *Arch. Pathol.*, **68**, 438–444.
13. Bethlem, J. and Vanwijngaarden, G.K. (1963) The incidence of ringed fibres and sarcoplasmic masses in normal and diseased muscle. *J. Neurol. Neurosurg. Psychiatry*, **26**, 326–332.
14. Pena, J., Luque, E., Noguera, F., Jimena, I. and Vaamonde, R. (2001) Experimental induction of ring fibers in regenerating skeletal muscle. *Pathol. Res. Pract.*, **197**, 21–27.
15. Engel, A.G. and Franzini-Armstrong, C. (2004) *Myology. Basic and Clinical*. McGraw-Hill, New York.
16. Muhlendyck, H. and Ali, S.S. (1978) Histological and ultrastructural studies on the ringbands in human extraocular muscles. *Albrecht Von Graefes Arch. Klin. Exp. Ophthalmol.*, **208**, 177–191.
17. Koenig, M., Hoffman, E.P., Bertelson, C.J., Monaco, A.P., Feener, C. and Kunkel, L.M. (1987) Complete cloning of the Duchenne muscular dystrophy (DMD) cDNA and preliminary genomic organization of the DMD gene in normal and affected individuals. *Cell*, **50**, 509–517.
18. Emery, A.E. (1990) Dystrophin function. *Lancet*, **335**, 1289.
19. Muntoni, F., Torelli, S. and Ferlini, A. (2003) Dystrophin and mutations: one gene, several proteins, multiple phenotypes. *Lancet Neurol.*, **2**, 731–740.
20. Banks, G.B., Fuhrer, C., Adams, M.E. and Froehner, S.C. (2003) The postsynaptic submembrane machinery at the neuromuscular junction: requirement for rapsyn and the utrophin/dystrophin-associated complex. *J. Neurocytol.*, **32**, 709–726.
21. Bhasin, N., Law, R., Liao, G., Safer, D., Ellmer, J., Discher, B.M., Sweeney, H.L. and Discher, D.E. (2005) Molecular extensibility of mini-dystrophins and a dystrophin rod construct. *J. Mol. Biol.*, **352**, 795–806.
22. Ervasti, J.M. (2007) Dystrophin, its interactions with other proteins, and implications for muscular dystrophy. *Biochim. Biophys. Acta.*, **1772**, 108–117.
23. Chamberlain, J.S. and Rando, T.A. (2006) *Duchenne Muscular Dystrophy. Advances in Therapeutics*. Taylor and Francis, NY.
24. Harper, S.Q., Hauser, M.A., DelloRusso, C., Duan, D., Crawford, R.W., Phelps, S.F., Harper, H.A., Robinson, A.S., Engelhardt, J.F., Brooks, S.V. *et al.* (2002) Modular flexibility of dystrophin: implications for gene therapy of Duchenne muscular dystrophy. *Nat. Med.*, **8**, 253–261.
25. Li, S., Kimura, E., Ng, R., Fall, B.M., Meuse, L., Reyes, M., Faulkner, J.A. and Chamberlain, J.S. (2006) A highly functional mini-dystrophin/GFP fusion gene for cell and gene therapy studies of Duchenne muscular dystrophy. *Hum. Mol. Genet.*, **15**, 1610–1622.
26. Law, D.J. and Tidball, J.G. (1993) Dystrophin deficiency is associated with myotendinous junction defects in prenecrotic and fully regenerated skeletal muscle. *Am. J. Pathol.*, **142**, 1513–1523.
27. Miosge, N., Klenczar, C., Herken, R., Willem, M. and Mayer, U. (1999) Organization of the myotendinous junction is dependent on the presence of alpha7beta1 integrin. *Lab. Invest.*, **79**, 1591–1599.
28. Deconinck, A.E., Rafael, J.A., Skinner, J.A., Brown, S.C., Potter, A.C., Metzinger, L., Watt, D.J., Dickson, J.G., Tinsley, J.M. and Davies, K.E. (1997) Utrophin-dystrophin-deficient mice as a model for Duchenne muscular dystrophy. *Cell*, **90**, 717–727.
29. Grady, R.M., Akaaboune, M., Cohen, A.L., Maimone, M.M., Lichtman, J.W. and Sanes, J.R. (2003) Tyrosine-phosphorylated and nonphosphorylated isoforms of alpha-dystrobrevin: roles in skeletal muscle and its neuromuscular and myotendinous junctions. *J. Cell Biol.*, **160**, 741–752.
30. Gregorevic, P., Blankinship, M.J., Allen, J.M., Crawford, R.W., Meuse, L., Miller, D.G., Russell, D.W. and Chamberlain, J.S. (2004) Systemic delivery of genes to striated muscles using adeno-associated viral vectors. *Nat. Med.*, **10**, 828–834.
31. Banks, G.B., Gregorevic, P., Allen, J.M., Finn, E.E. and Chamberlain, J.S. (2007) Functional capacity of dystrophins carrying deletions in the N-terminal actin-binding domain. *Hum. Mol. Genet.*, **16** (17), 2105–2113.
32. Fidzianska, A. and Kaminska, A. (2003) Congenital myopathy with abundant ring fibres, rimmed vacuoles and inclusion body myositis-type inclusions. *Neuropediatrics*, **34**, 40–44.
33. Sawicka, E. (1991) Origin of the ring muscle fibers in neuromuscular diseases. *Neuropatol. Pol.*, **29**, 29–40.
34. Street, S.F. (1983) Lateral transmission of tension in frog myofibers: a myofibrillar network and transverse cytoskeletal connections are possible transmitters. *J. Cell. Physiol.*, **114**, 346–364.
35. Bloch, R.J. and Gonzalez-Serratos, H. (2003) Lateral force transmission across costameres in skeletal muscle. *Exerc. Sport Sci. Rev.*, **31**, 73–78.
36. Passerieux, E., Rossignol, R., Letellier, T. and Delage, J.P. (2007) Physical continuity of the perimysium from myofibers to tendons: involvement in lateral force transmission in skeletal muscle. *J. Struct. Biol.*, **159**, 19–28.
37. Lynch, G.S. (2004) Role of contraction-induced injury in the mechanisms of muscle damage in muscular dystrophy. *Clin. Exp. Pharmacol. Physiol.*, **31**, 557–561.
38. Gregorevic, P., Allen, J.M., Minami, E., Blankinship, M.J., Haraguchi, M., Meuse, L., Finn, E., Adams, M.E., Froehner, S.C., Murry, C.E. *et al.* (2006) rAAV6-microdystrophin preserves muscle function and extends lifespan in severely dystrophic mice. *Nat. Med.*, **12**, 787–789.
39. Matsuda, R., Nishikawa, A. and Tanaka, H. (1995) Visualization of dystrophic muscle fibers in mdx mouse by vital staining with Evans blue: evidence of apoptosis in dystrophin-deficient muscle. *J. Biochem. (Tokyo)*, **118**, 959–964.
40. Mankodi, A., Logigian, E., Callahan, L., McClain, C., White, R., Henderson, D., Krym, M. and Thornton, C.A. (2000) Myotonic dystrophy in transgenic mice expressing an expanded CUG repeat. *Science*, **289**, 1769–1773.
41. Cho, D.H. and Tapscott, S.J. (2007) Myotonic dystrophy: emerging mechanisms for DM1 and DM2. *Biochim. Biophys. Acta.*, **1772**, 195–204.
42. Wheeler, T.M. and Thornton, C.A. (2007) Myotonic dystrophy: RNA-mediated muscle disease. *Curr. Opin. Neurol.*, **20**, 572–576.
43. Nagao, H., Morimoto, T., Sano, N., Takahashi, M., Nagai, H., Tawa, R., Yoshimatsu, M., Woo, Y.J. and Matsuda, H. (1991) Magnetic resonance imaging of skeletal muscle in patients with Duchenne muscular dystrophy – serial axial and sagittal section studies. *No To Hattatsu*, **23**, 39–43.
44. Hasegawa, T., Matsumura, K., Hashimoto, T., Ikehira, H., Fukuda, H. and Tateno, Y. (1992) Intramuscular degeneration process in Duchenne muscular dystrophy – investigation by longitudinal MR imaging of the skeletal muscles. *Rinsho Shinkeigaku*, **32**, 333–335.
45. Ervasti, J.M. (2003) Costameres: the Achilles' heel of Herculean muscle. *J. Biol. Chem.*, **278**, 13591–13594.
46. Bloch, R.J., Reed, P., O'Neill, A., Strong, J., Williams, M., Porter, N. and Gonzalez-Serratos, H. (2004) Costameres mediate force transduction in healthy skeletal muscle and are altered in muscular dystrophies. *J. Muscle Res. Cell Motil.*, **25**, 590–592.
47. Kaariainen, M., Nissinen, L., Kaufman, S., Sonnenberg, A., Jarvinen, M., Heino, J. and Kalimo, H. (2002) Expression of alpha7beta1 integrin splicing variants during skeletal muscle regeneration. *Am. J. Pathol.*, **161**, 1023–1031.
48. Katsumi, A., Naoe, T., Matsushita, T., Kaibuchi, K. and Schwartz, M.A. (2005) Integrin activation and matrix binding mediate cellular responses to mechanical stretch. *J. Biol. Chem.*, **280**, 16546–16549.
49. Song, W.K., Wang, W., Foster, R.F., Bielser, D.A. and Kaufman, S.J. (1992) H36-alpha 7 is a novel integrin alpha chain that is developmentally regulated during skeletal myogenesis. *J. Cell Biol.*, **117**, 643–657.
50. Blake, D.J., Tinsley, J.M. and Davies, K.E. (1996) Utrophin: a structural and functional comparison to dystrophin. *Brain Pathol.*, **6**, 37–47.
51. Khurana, T.S., Watkins, S.C., Chafey, P., Chelly, J., Tome, F.M., Fardeau, M., Kaplan, J.C. and Kunkel, L.M. (1991) Immunolocalization and developmental expression of dystrophin related protein in skeletal muscle. *Neuromuscul. Disord.*, **1**, 185–194.
52. Ohlendieck, K., Ervasti, J.M., Matsumura, K., Kahl, S.D., Leveille, C.J. and Campbell, K.P. (1991) Dystrophin-related protein is localized to neuromuscular junctions of adult skeletal muscle. *Neuron*, **7**, 499–508.
53. Pons, F., Augier, N., Leger, J.O., Robert, A., Tome, F.M., Fardeau, M., Voit, T., Nicholson, L.V., Mornet, D. and Leger, J.J. (1991) A homologue of dystrophin is expressed at the neuromuscular junctions of normal individuals and DMD patients, and of normal and mdx mice. Immunological evidence. *FEBS Lett.*, **282**, 161–165.
54. Grady, R.M., Merlie, J.P. and Sanes, J.R. (1997) Subtle neuromuscular defects in utrophin-deficient mice. *J. Cell Biol.*, **136**, 871–882.
55. Sadoulet-Puccio, H.M., Rajala, M. and Kunkel, L.M. (1997) Dystrobrevin and dystrophin: an interaction through coiled-coil motifs. *Proc. Natl Acad. Sci. USA*, **94**, 12413–12418.
56. Crawford, G.E., Faulkner, J.A., Crosbie, R.H., Campbell, K.P., Froehner, S.C. and Chamberlain, J.S. (2000) Assembly of the dystrophin-associated protein complex does not require the dystrophin COOH-terminal domain. *J. Cell. Biol.*, **150**, 1399–1410.

57. Martinez, A.J., Hay, S. and McNeer, K.W. (1976) Extraocular muscles: light microscopy and ultrastructural features. *Acta Neuropathol.*, **34**, 237–253.
58. McKelvie, P., Friling, R., Davey, K. and Kowal, L. (1999) Changes as the result of ageing in extraocular muscles: a post-mortem study. *Aust. N Z J. Ophthalmol.*, **27**, 420–425.
59. Rafael, J.A., Cox, G.A., Corrado, K., Jung, D., Campbell, K.P. and Chamberlain, J.S. (1996) Forced expression of dystrophin deletion constructs reveals structure-function correlations. *J. Cell Biol.*, **134**, 93–102.
60. Burkholder, T.J., Fingado, B., Baron, S. and Lieber, R.L. (1994) Relationship between muscle fiber types and sizes and muscle architectural properties in the mouse hindlimb. *J. Morphol.*, **221**, 177–190.
61. Straub, V., Rafael, J.A., Chamberlain, J.S. and Campbell, K.P. (1997) Animal models for muscular dystrophy show different patterns of sarcolemmal disruption. *J. Cell Biol.*, **139**, 375–385.